Journal of Statistical Physics, Vol. 26, No. 3, 1981

Correlations and Spectra of Periodic Chaos Generated by the Logistic Parabola

Stefan Thomae[1] and Siegfried Grossmann[1]

Received January 5, 1981

We consider the one-parameter family of mappings $f_a(x) = 4ax(1-x)$, $a, x \in [0, 1]$ and define an infinite countable set of parameter values $\tilde{a}$ for which the solutions show observable chaos. Their properties are investigated by means of correlation functions and spectra, which can be interpreted and approximated by separating periodic and chaotic components in the solutions and introducing two simple assumptions on the statistics of the chaotic component.

KEY WORDS: Recurrence; bifurcation; limit cycle; logistic equation; chaos; correlation function; spectrum; noise.

1. INTRODUCTION

In recent years there has been considerable progress in the understanding of the dynamic properties of discrete nonlinear one-dimensional dynamic systems[1-8]

$$x_{\tau+1}(a) = f_a(x_\tau(a)), \qquad a \in J, \qquad x_\tau \in I, \qquad \tau = 0, 1, 2, \ldots \tag{1}$$
$$\text{with } f_a : I \leftarrow\!\!\supset, \; I, J: \text{ intervals of the real axis}$$

Concerning applications[9-20] to experimentally realizable systems the *stable stationary* dynamics generated by f_a is of particular interest. The stationary dynamics is characterized by the asymptotic behavior of typical solutions $\{x_\tau(a)\}_{\tau=0}^{\infty}$ of (1) which is either periodic or chaotic. A solution is typical if the set of initial points x_0 giving rise to solutions with the same asymptotic behavior is not countable. By the stability of the dynamics we mean that the solutions considered do not change their type of behavior under infinitesimal perturbations. This requirement is essential for the comparability with experimental results, which are usually obtained in the

[1] Fachbereich Physik, Philipps-Universität, Renthof 6, D-3550 Marburg, Germany.

0022-4715/81/1100-0485$03.00/0

presence of some background noise. In the case of periodic solutions the problem of stability is easily resolved by a linear stability analysis, see, e.g., Ref. 20. In the chaotic case, however, one is led to the important question of observability.[21] Many numerical investigations corroborate that the Li–Yorke criterion[22] only states the formal existence of chaos but not its observability. Oono and Takahashi[21] investigated this point and proposed a criterion for the observability of chaos.

In this paper we consider as an example for (1) the logistic parabola

$$f_a(x) = 4ax(1-x), \qquad a, x \in [0,1] \tag{2}$$

which has the advantage of combining the capacity of a multitude of generic features with a comparatively simple mathematical form.

After reviewing some results needed later (Section 2), we describe how one can obtain for each stable periodic solution a corresponding state of periodic chaos (Section 3). This procedure can also be applied to dynamical laws other than (2). In Sections 4 and 5 we discuss the correlation functions and spectra in these states. While the correlations are very well suited to recognize chaotic states as closely related, e.g., a cycle and its subharmonic, the spectra render a clear-cut discrimination even between those closely related states. An approximation method for the spectra relying on a decomposition of the dynamics into a periodic and a pseudostochastic component is proposed in Section 6.

2. STABLE DYNAMICS

For $a \in [0, a_c^{(1)})$, $a_c^{(1)} = 0.892\,486\,417\ldots$ the typical solutions of (2) show asymptotically periodic behavior with period $p = 2^{n(a)}$, $n(a) = 0, 1, 2, \ldots$. The solutions converge to limit sets $\Lambda(a) = \{\hat{x}_j(a)\}_{j=0}^{p-1}$ with $\hat{x}_{j+1} = f_a(\hat{x}_j)$ for $j = 0, 1, 2, \ldots, p-2$ and $\hat{x}_0 = f_a(\hat{x}_{p-1})$; $\hat{x}_0(a) > \hat{x}_j(a)$, $j = 1, 2, 3, \ldots, p-1$.

For $a \in (a_c^{(1)}, 1]$ Hoppensteadt and Hyman[23] demonstrated the existence of formal chaos by applying the Li–Yorke criterion to iterated maps $f_a^{(n)} = f_a \circ f_a^{(n-1)}$, $f_a^{(0)}(x) \equiv x$. $a_c^{(1)}$ thus plays the role of a critical point separating an "ordered phase" ($a < a_c^{(1)}$), where periodic solutions with periods $p = 2^{n(a)}$ prevail, from a "disordered" one ($a > a_c^{(1)}$) characterized by formal chaos.[24,25] The analogy to a continuous (second-order) phase transition can even be carried further. The bifurcation points $a_n^{(1)} < a_c^{(1)}$, $n = 1, 2, 3, \ldots$ where the period of stable solutions jumps from $p = 2^{n-1}$ to $p = 2^n$ obey asymptotically an exponential law[26,2]

$$a_n^{(1)} \underset{n\to\infty}{\simeq} a_c^{(1)} - a^{(1)}\delta^{-n} \tag{3}$$

Feigenbaum[2,3] (who considered the points of maximum cycle stability) obtained by high precision computations $\delta = 4.669\,201\,609\,102\ldots$. The empirical observation of exponential convergence was put on a sound mathematical basis by proofs of Collet *et al.*[4] and Lanford III.[27]

For $a = a_c^{(1)}$ the limit set $\Lambda(a_c^{(1)})$ is a Cantor set.[28,29,4] According to Ref. 13 it can be described as the limit obtained by iterated fragmentation into subintervals with scaling factors $-1/\alpha$ and $1/\alpha^2$ where $\alpha = 2.502\,907\,875\ldots$.[2,3] In our own numerical computations (accuracy: ten decimal places) we have found α to vary within $[2.356, 2.577]$.

In the interval $(a_c^{(1)}, 1]$ further stable periodic solutions (cycles) occur showing a behavior analogous to that observed in $[0, a_c^{(1)})$: At some value $a_0^{(m)}$ a primary cycle of period m comes into existence by "tangent-type" bifurcation[20] (called "saddle node" in Ref. 30). If a is increased, the primary cycle finally loses stability and subharmonics of period $p = m \cdot 2^n$, $n = 1, 2, 3, \ldots$ consecutively become stable at parameter values $a_n^{(m)}$. They are generated by "slope-type" bifurcation[20] (called "flip" in Ref. 30). Again the series $\{a_n^{(m)}\}_{n=0}^{\infty}$, $m = 3, 4, 5, \ldots$ converge to critical values $a_c^{(m)}$ asymptotically obeying exponential laws

$$a_n^{(m)} \underset{n\to\infty}{\simeq} a_c^{(m)} - a^{(m)}\delta^{-n} \tag{4}$$

with the same δ as in (3). For $m \geqslant 5$ there is more than one primary cycle for each m. These cycles differ in the ordering of periodic points.[31] An explicit formula for the multiplicity of cycles as function of m is given in Ref. 32. To keep track of different cycles with the same period we introduce a new index $r \geqslant 1$. Thereby we adopt the convention $r_1 < r_2$ if $a_0^{(m,r_1)} < a_0^{(m,r_2)}$.

Defining $J^{(m,r)} = [a_0^{(m,r)}, a_c^{(m,r)})$ we have $J^{(m_1,r_1)} \cap J^{(m_2,r_2)} = \emptyset$ if $(m_1, r_1) \neq (m_2, r_2)$ as a consequence of a theorem of Fatou[33] and Julia[34] stating that two different cycles cannot be stable simultaneously.

The theorem of Šarkovskii[35,36] gives an order relation between different $J^{(m,r)}$ which corresponds to the order relation of Metropolis, Stein, and Stein[31] (MSS), later amended by Collet and Eckmann.[5,8] They developed the following procedure to characterize the structure of stable cycles:

For each stable cycle there is a value of a for which it is superstable, i.e., the point $x^* = 1/2$ with $f_a'(x = x^*) = 0$ is element of the limit set $\Lambda(a)$. With $\hat{x}_{p-1}(a) = x^*$ the cycle structure is characterized by describing the position of each $\hat{x}_j(a)$ relative to $\hat{x}_{p-1}(a)$ for $j = 0, 1, 2, \ldots, p-2$ by symbols R and L, where R denotes the case $\hat{x}_j(a) > x^*$ and L the case $\hat{x}_j(a) < x^*$. Thus each cycle is labeled by a sequence of Rs and Ls. Although the periodic points $\hat{x}_j(a)$ shift as functions of a, the ordering described by these MSS sequences stays the same as long as the cycle in question exists.

Interpreting R and L as branches of the inverse map $f_a^{(-1)}$

$$R_a(x) = \left[1 + (1 - x/a)^{1/2}\right]/2 \qquad \text{right branch}$$

$$L_a(x) = \left[1 - (1 - x/a)^{1/2}\right]/2 \qquad \text{left branch}$$

these sequences lead to a straightforward numerical procedure to determine the parameter values $\hat{a}_n^{(m,r)}$ of maximum cycle stability. Let $\mathcal{P}$ denote a given MSS sequence $RL\ldots$. Then the corresponding $\hat{a}_n^{(m,r)}$ is a solution of $\hat{a} = P_{\hat{a}}(1/2)$ where P_a denotes the function $R_a \circ L_a \circ \cdots$.

Another useful means for the description of cycle structures is the following composition law[37]:

If $\mathcal{P}$ and $\mathcal{Q} = \sigma_0\sigma_1\sigma_2 \cdots \sigma_q$, $\sigma_j = R, L$ are two MSS sequences, $\mathcal{P}*\mathcal{Q}$ is the sequence $\mathcal{P}\tau_0\mathcal{P}\tau_1 \cdots \mathcal{P}\tau_{q-1}\mathcal{P}\tau_q\mathcal{P}$ with $\tau_j = R, L$ and

$$\tau_j \begin{cases} = \sigma_j & \text{if } \mathcal{P} \text{ has an even number of } R \text{ characters} \\ \neq \sigma_j & \text{otherwise} \end{cases}$$

Thus, for example, the bifurcation of a cycle $\mathcal{P}$ into a series of subharmonics is described by $\mathcal{P}*R^{*n}$, $n = 1, 2, 3, \ldots$. (Note: $R^3 = RRR$, but $R^{*3} = R*R*R$).

3. STATES OF PERIODIC CHAOS

Starting from a cycle of period p, which becomes stable at $a = a_n^{(m,r)}$, one can find a parameter value where chaos is observable by proceeding as follows:

(i) One adjusts a to the value $\hat{a}_n^{(m,r)}$ where the cycle in question is superstable (Fig. 1a).

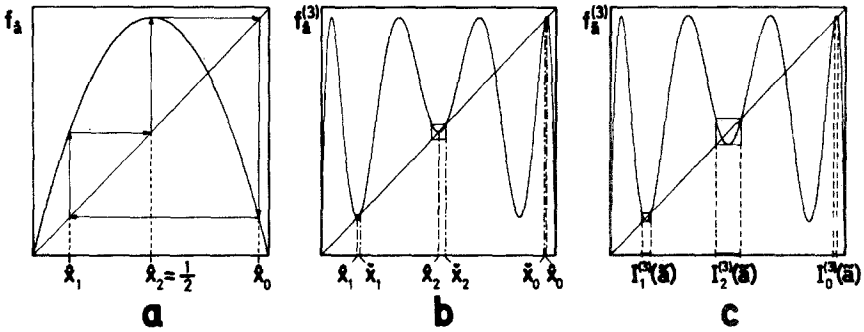

Fig. 1. Construction of states of periodic chaos. (a) Superstable cycle of $f_{\hat{a}}$; (b) periodic points show up as stable fixed points in the p-fold iterated map at the same parameter value $\hat{a}$; (c) f_1-like situation in each box after a slight increase of the parameter to a value $\tilde{a}$.

(ii) Each periodic point $\hat{x}_j(a)$ shows up as a stable fixed point of the iterated map $f_a^{(p)}$ (Fig. 1b). In the neighborhood of each of them there is an unstable fixed point $\check{x}_j(a)$ coinciding with the stable one for $a = a_n^{(m,r)}$. Using these neighboring fixed points as corner points one can construct squares around all stable fixed points in the manner indicated in Fig. 1b. These squares define intervals $I_j^{(p)}(a)$ which are mapped *in*to themselves by $f_a^{(p)}$.

(iii) Increasing a one finally arrives at $a = \tilde{a}_n^{(m,r)}$, where $f_a^{(p)}$ maps all $I_j^{(p)}(a)$ *on*to themselves, i.e., on each square the local extremum of $f_a^{(p)}$ touches the lower or upper edge (Fig. 1c).

Figure 2 shows some examples obtained this way. Some values for $\tilde{a}_n^{(m,r)}$ are given in Table I.

In the following we discuss the dynamic properties of such states by means of correlation functions and spectra. A thorough account on other aspects of these states is given in Ref. 6 and their invariant densities are discussed in Refs. 38–42. Within each of the squares, i.e., on intervals

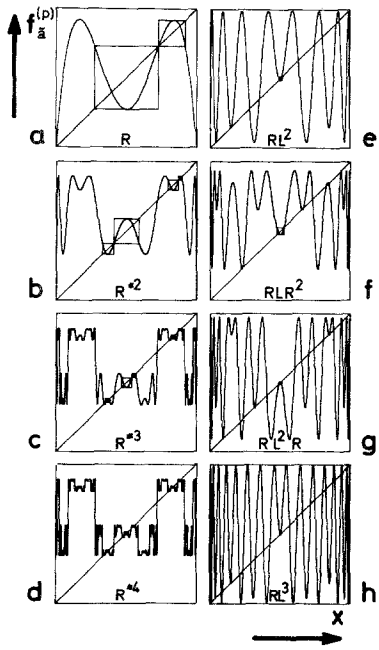

Fig. 2. States of periodic chaos. The diagrams show the respective iterated maps $f_{\tilde{a}}^{(p)}$ on the unit square with chaotic boxes. (a)–(d) Subharmonics of $p = 1$; in going from a cycle to its subharmonic each box is replaced by a pair of linked boxes; (e)–(h) primary cycles, boxes are far apart from each other; (f)–(h) show different period-5 chaotic states.

Table I. Parameter Values for Some States of Periodic Chaos

MSS	m	r	n	$\tilde{a}_n^{(m,r)}$
	1	1	0	1.000 000 000
R			1	0.919 643 377 · · ·
R^{*2}			2	0.898 143 046 · · ·
R^{*3}			3	0.893 701 234 · · ·
R^{*4}			4	0.892 746 485 · · ·
$R^{*\infty}$			∞	0.892 486 417 · · ·
RL	3	1	0	0.964 200 163 · · ·
$RL*R$			1	0.962 782 093 · · ·
$RL*R^{*2}$			2	0.962 446 111 · · ·
$RL*R^{*\infty}$			∞	0.962 358 420 · · ·
RLL	4	1	0	0.990 398 880 · · ·
$RLL*R$			1	0.990 322 998 · · ·
$RLRR$	5	1	0	0.936 177 583 · · ·
$RLRR*R$			1	0.935 853 583 · · ·
$RLLR$	5	2	0	0.976 693 038 · · ·
$RLLR*R$			1	0.976 632 301 · · ·
$RLLL$	5	3	0	0.997 586 178 · · ·
$RLLL*R$			1	0.997 581 743 · · ·

$I_j^{(p)}(\tilde{a})$, $j = 0, 1, 2, \ldots, p-1$, the map $f_{\tilde{a}}^{(p)}$ generates a dynamics analogous to that of f_1 on the unit interval. Therefore observable chaos is expected in each of these boxes. As Misiurewicz[42] could show, these states indeed have invariant ergodic measures $\mu^{(p)}(dx)$ absolutely continuous with respect to the Lebesgue measure. Numerical studies[38,39] indicate their observability.[21,43]

An example of a solution of f_a for $a = \tilde{a}_n^{(m,r)}$ is given in Fig. 3b. The qualitative behavior is easily understood as the superposition of the chaotic solutions within the squares and the periodic mapping of the squares onto each other (Fig. 3a). Therefore we called these states "periodically chaotic" in Ref. 26. Other authors use the term "semiperiodic"[44] or characterize these states by the occurrence of "invariant segments".[7]

Obviously there is exactly one $\tilde{a}_n^{(m,r)}$ for each $a_n^{(m,r)}$, i.e., to each stable cycle there is exactly one state of periodic chaos. Therefore we also use the RL pattern of the underlying cycle to label the corresponding chaotic state. Because of this one-to-one relation between stable cycles and states of periodic chaos the set $\{\tilde{a}_n^{(m,r)}\}$ is infinite but countable. General considerations, however, indicate that the set of parameter values leading to

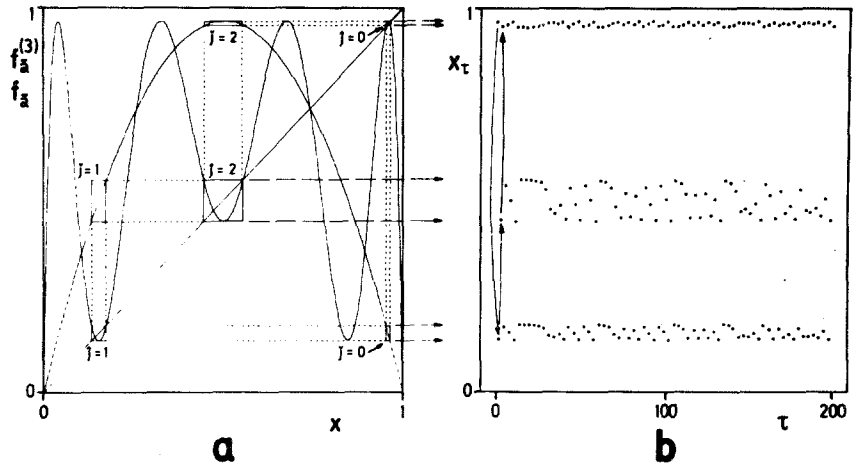

Fig. 3. Superposition of periodic and pseudostochastic components for $a = \tilde{a}_0^{(3,1)}$. (a) Within each box $j = 0, 1, 2$ on the diagonal $f_{\tilde{a}}^{(3)}$ generates a chaotic solution; $f_{\tilde{a}}$ maps the chaotic boxes onto each other in a cyclic fashion; only those parts of $f_{\tilde{a}}$ contained in the off-diagonal boxes $j = 0, 1, 2$ become effective; (b) solution of $f_{\tilde{a}}$; the chaotic behavior within each box is obvious.

observable chaos has positive Lebesgue measure.[8] Up to now no proof of this is available.

The order relation between different cycles[31,5] can likewise be used to give an ordering of different states of periodic chaos. To this end we consider first the case $a = \tilde{a}_0^{(1,1)} = 1$. Let $a(\mathcal{P})$ denote the value of the parameter where the cycle $\mathcal{P}$ is superstable. Then

$$\tilde{a}_0^{(1,1)} = \lim_{\gamma \to \infty} a(RL^\gamma) \tag{5}$$

To prove the validity of this equation we interpret R and L as inverse operators of f_a as in Section 2. Since L has only one globally stable fixed point at zero, $L^{(\gamma)}(1/2) \to 0$ for $\gamma \to \infty$ and $R(0) = 1$.

In the more general case of a periodic chaos with an underlying cycle $\mathcal{P}_n^{(m,r)} = \mathcal{P}_0^{(m,r)} * R^{*n}$ the corresponding value $\tilde{a}_n^{(m,r)}$ is given by

$$\tilde{a}_n^{(m,r)} = \lim_{\gamma \to \infty} a(\mathcal{P}_n^{(m,r)} * RL^\gamma) \qquad \text{for each } (m,r), n \tag{6}$$

This relation is easily understood by taking into account that in $\mathcal{P} * \mathcal{Q}$ the first sequence $\mathcal{P}$ describes the overall structure of the cycle, whereas $\mathcal{Q}$ describes its fine structure.[37] The limit $\gamma \to \infty$ in $*RL^\gamma$ thus makes the local extrema of $f_a^{(p)}$ approach the edges of the respective squares while $\mathcal{P}_n^{(m,r)}$ takes care of the coarse cycle structure. A proof of (6) can again be given by interpreting R and L as inverse maps. Thus by using the order relation between MSS sequences[31,5] one arrives at an ordering for the

$\tilde{a}_n^{(m,r)}$. Another conclusion drawn from the order relation between MSS sequences is

$$\lim_{n\to\infty} a_n^{(m,r)} = \lim_{n\to\infty} \tilde{a}_n^{(m,r)} \qquad \text{for each } (m,r) \tag{7}$$

Both limits are equal because the sequences $\lim_{n\to\infty} \mathcal{P}_0^{(m,r)} * R^{*n}$ and $\lim_{n\to\infty} \lim_{\gamma\to\infty} \mathcal{P}_0^{(m,r)} * R^{*n} * RL^{\gamma}$ agree for an infinite number of consecutive symbols from the start. A full-fledged general proof is given by Collet *et al.*[4] The $\tilde{a}_n^{(m,r)}$, $n = 0, 1, 2, \ldots$ again obey an asymptotic exponential law[26,39,4]

$$\tilde{a}_n^{(m,r)} \underset{n\to\infty}{\simeq} a_c^{(m,r)} + \tilde{a}^{(m,r)}\delta^{-n} \qquad \text{for each } (m,r) \tag{8}$$

where δ is again the same as in (3).

4. CORRELATIONS IN STATES OF PERIODIC CHAOS

A more detailed description of periodic chaos is obtained by use of correlation functions (c.f.) defined as

$$c_\tau(\tilde{a}) = \langle \delta x(\tilde{a}) \delta x_\tau(\tilde{a}) \rangle \tag{9}$$

with the fluctuation

$$\begin{aligned} \delta x_\tau(\tilde{a}) &= x_\tau(\tilde{a}) - \langle x(\tilde{a}) \rangle \\ \delta x(\tilde{a}) &= \delta x_{\tau=0}(\tilde{a}) \end{aligned} \tag{10}$$

The average $\langle \cdots \rangle$ may be calculated either as

$$\text{ensemble average } \langle \cdots (x) \rangle = \int_0^1 \cdots (x)\, d\mu^{(p)}(x)$$

or as

$$\text{time average } \langle \cdots (x_t) \rangle = \lim_{T\to\infty} \frac{1}{T} \sum_{t=0}^{T-1} \cdots (x_t)$$

since ergodicity is given (Section 3).

For $a = \tilde{a}_0^{(1,1)} = 1$ the c.f. can be calculated analytically,[26,39]

$$c_\tau(1) = \begin{cases} 0.125 & \text{if } \tau = 0 \\ 0 & \text{if } \tau \neq 0 \end{cases} \tag{11}$$

Numerical results for other values of a are shown in Fig. 4. In all cases the c.f.'s rapidly converge with increasing τ to a periodic oscillation. Decomposing the complete solution $\{x_\tau(\tilde{a}^{(p)})\}_{\tau=0}^{\infty}$ into p subsolutions $\{x_\tau^{(j)}(\tilde{a}^{(p)})\}_{\tau=0}^{\infty}$, $j = 0, 1, 2, \ldots, p-1$, where the jth subsolution is completely contained in the jth chaotic box, this asymptotic oscillation is easily

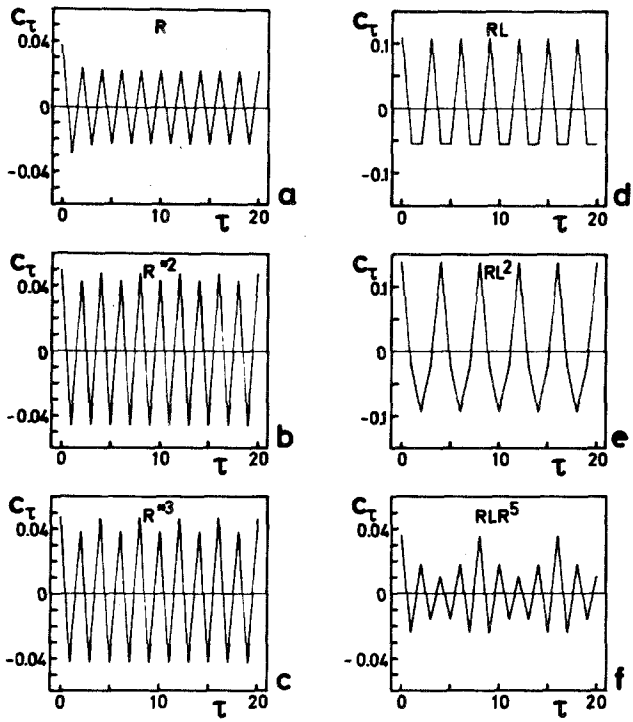

Fig. 4. Correlation functions for several states of periodic chaos (time average with $T = 50{,}000$); aside from a slight change in amplitude c differs from b also in an additional periodic oscillation of the amplitudes, which, however, is so small that it cannot be discerned in c.

explained as the c.f. of the mean values of subsolutions. Thus, a different structure of the underlying cycle in general shows up clearly in the asymptotic behavior of the c.f.'s. Compare for example Figs. 4b, 4c with Figs. 4e, 4f, both showing c.f.'s in states of chaos with $p = 4$ and $p = 8$, respectively. On the other hand the close structural similarity between a cycle and its subharmonics leads to similarly looking c.f.'s (Figs. 4a–4c).

The investigation of the dynamic behavior in a single box generated by the iterated map $f_{\tilde{a}}^{(p)}$ reveals another interesting feature. Therefore we consider the subsolutions $\{x_\tau^{(j)}(\tilde{a}^{(p)})\}_{\tau=0}^{\infty}$. To facilitate a comparison with the c.f. for $a = 1$ we normalize all of these solutions to the unit interval by

$$\tilde{x}_\tau^{(j)} = \left(x^{(j)} - \check{x}_j\right)/l_j \tag{12}$$

where l_j is the length of $I_j^{(p)}(\tilde{a})$ multiplied by $+1(-1)$ if $f_{\tilde{a}}^{(p)}$ has a local

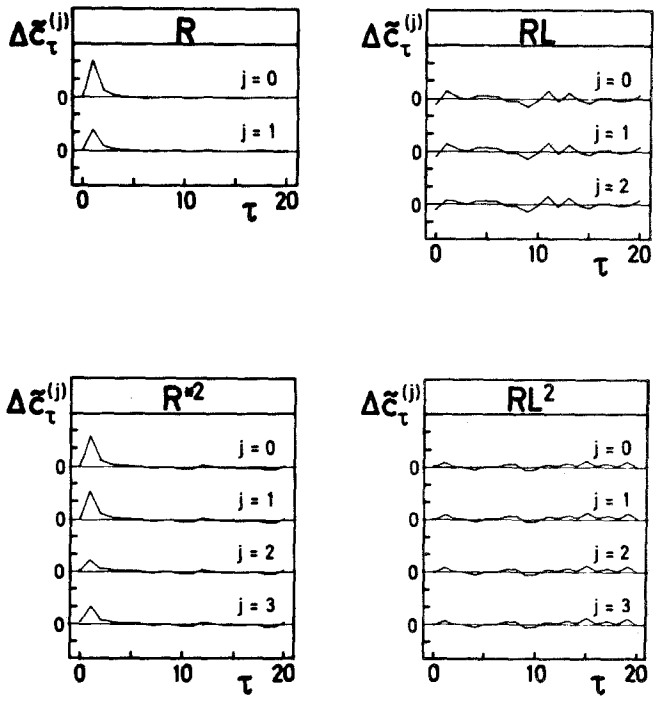

Fig. 5. Deviation $\Delta\tilde{c}_\tau^{(j)}$ of correlation functions in normalized boxes from "normal" behavior (time average with $T = 50{,}000$); one ordinate unit = 0.01.

maximum (minimum) in $I_j^{(p)}(\tilde{a})$. The box c.f.'s

$$\tilde{c}_\tau^{(j)}(\tilde{a}) = \left\langle \delta\tilde{x}^{(j)}(\tilde{a})\delta\tilde{x}_\tau^{(j)}(\tilde{a}) \right\rangle \tag{13}$$

are similar to the "normal" c.f. (11). Since we are interested in the deviations from (11), we consider the difference $\Delta\tilde{c}_\tau^{(j)}(\tilde{a}) = \tilde{c}_\tau^{(j)}(\tilde{a}) - c_\tau(1)$, see Fig. 5.

The numerical results may be summarized by the following rule: If the underlying cycle is primary in the sense of Section 2, the box c.f.'s decay almost as fast as $c_\tau(1)$. If the underlying cycle is a subharmonic, the decay is appreciably slower. In all cases the decay is monotonous.

We pointed out in Ref. 26 that the immediate decay as observed in (11) is brought about by an intricate balance in the shape of the dynamical law. The dynamic law f_a considered here as well as all iterated maps $f_a^{(p)}$ are polynomials. Since the first derivative f_a' has only one zero at $x^* = 1/2$, it is clear from the construction of the $\tilde{a}_n^{(m,r)}$ that in the case of period-p chaos the first derivative of $f_{\tilde{a}}^{(p)}$ has precisely one zero z_j of first order in

each chaotic box j. Denoting the other zeros of $f_a^{(p)}(x)$, which is a polynomial of $(2^p - 1)$th degree, by $z_p, z_{p+1}, \ldots, z_{2^p-2}$, $f_a^{(p)'}(x)$ can be represented by $\prod_{k=0}^{2^p-2}(x - z_k)$. The deviation of $f_a^{(p)}$ from a parabolic shape in the box j can be measured by the ratio

$$r_j = \min_{k \neq j} |z_j - z_k| / |l_j|, \qquad k = 0, 1, 2, \ldots, 2^p - 2 \tag{14}$$

This is because $r_j \gg 1$ means $f_a^{(p)'}(x)$ is almost linear in box j and therefore $f_a^{(p)}(x)$ is almost parabolic:

$$f_a^{(p)'}(x) = \prod_{k=0}^{2^p-2}(x - z_k) \quad \propto (x - z_j) \qquad \text{for } x \in I_j^{(p)}, \quad r_j \gg 1$$

$$f_a^{(p)}(x) \qquad\qquad \propto \tfrac{1}{2}x^2 - z_j x + \text{const} \qquad \text{for } x \in I_j^{(p)}, \quad r_j \gg 1$$

Table II contains the values of r_j for the box c.f.'s shown in Fig. 5. $r_j \gg 1$ clearly implies a close to normal behavior of the respective box c.f. whereas the converse is not true.

Thus the observed slower decay of box c.f.'s in the case of subharmonic underlying cycles is a probable but not necessary consequence of the pairing of boxes occurring in this case (Figs. 2a–2d). On the other hand, boxes are always isolated if the underlying cycle is a primary one (Figs. 2e–2h), which accounts for the close similarity of the box c.f.'s to $c_\tau(1)$.

Table II. Shape Parameter r_j for Subharmonics and Primary Cycles

Cycle	j	r_j
R	0	1.76
	1	0.74
R^{*2}	0	1.78
	1	1.67
	2	0.69
	3	0.75
RL	0	9.61
	1	2.72
	2	1.59
RLL	0	44.9
	1	11.6
	2	6.73
	3	3.37

5. SPECTRA OF PERIODIC CHAOS

In this section we consider the power spectra of periodically chaotic solutions using the discrete Fourier transformation. To avoid ambiguities in this formalism we introduce the concept of the "N-truncated" solution as follows:

If $\{x_\tau\}_{\tau=0}^{\infty}$ is a solution of (1), then $\{x_{\tau,N}\}_{\tau=0}^{\infty}$ with $x_{\tau,N} = x_\tau$ for $\tau = 0, 1, 2, \ldots, N-1$ and $x_{\tau+N,N} = x_{\tau,N}$, $\tau = 0, 1, 2, \cdots$ is referred to as "N-truncated" solution.[2]

Its c.f.

$$c_{\tau,N} = \langle \delta x_{0,N} \delta x_{\tau,N} \rangle \tag{15}$$

can be obtained from the c.f. c_τ of the original solution by

$$c_{\tau,N} = (1 - \tau/N)c_\tau + (\tau/N)c_{N-\tau}, \qquad \tau = 0, 1, 2, \ldots, N \tag{16}$$

For $\tau \ll N$ we have $c_{\tau,N} \cong c_\tau$. If c_τ decays in a characteristic time τ_c and $N \gg \tau_c$, $c_{\tau,N}$ may be looked upon as a good approximation to c_τ, and N truncation can be regarded as mere technicality.

We define the Fourier transform of the fluctuations of an "N-truncated" solution $\{x_{\tau,N}\}_{\tau=0}^{\infty}$ as

$$X_{\nu,N} = \frac{1}{N} \sum_{\tau=0}^{N-1} \exp(-i2\pi\nu\tau/N)\delta x_{\tau,N}, \qquad \nu = 0, 1, 2, \ldots, N-1 \tag{17}$$

The inverse transformation is

$$\delta x_{\tau,N} = \sum_{\nu=0}^{N-1} \exp(i2\pi\tau\nu/N)X_{\nu,N}, \qquad \tau = 0, 1, 2, \ldots, N-1 \tag{18}$$

Since the fluctuations $\delta x_{\tau,N}$ are real, the Fourier transform has the property

$$X_{N-\nu,N} = \bar{X}_{\nu,N} \tag{19}$$

where the overbar denotes the complex conjugate. Introducing (18) into (15) we obtain

$$c_{\tau,N} = \langle \delta x_{t,N} \delta x_{t+\tau,N} \rangle$$

$$c_{\tau,N} = \sum_{\mu=0}^{N-1} \sum_{\nu=0}^{N-1} \exp\{i2\pi[t(\mu+\nu) + \tau\nu]/N\} \langle X_{\mu,N} X_{\nu,N} \rangle$$

Since the fluctuations $\delta x_{t,N}$ are stationary, $c_{\tau,N}$ does not depend on t, i.e.,

$$\langle X_{\mu,N} X_{\nu,N} \rangle = 0 \text{ if } \mu + \nu \neq 0 \pmod{N} \tag{20}$$

[2]Note that "N-truncated" is just short for "truncated to N elements and then periodically continued."

Therefore

$$c_{\tau,N} = \sum_{\nu=0}^{N-1} \exp(i2\pi\tau\nu/N)\langle X_{N-\nu}, X_{\nu,N}\rangle$$

and because the fluctuations are real, we have

$$c_{\tau,N} = \sum_{\nu=0}^{N-1} \exp(i2\pi\tau\nu/N) S_{\nu,N} \tag{21}$$

$$S_{\nu,N} = \frac{1}{N} \sum_{\tau=0}^{N-1} \exp(-i2\pi\nu\tau/N) c_{\tau,N} \tag{22}$$

where

$$S_{\nu,N} = \langle |X_{\nu,N}|^2 \rangle \tag{23}$$

is the power spectrum.

Introducing (11) into (22) we obtain for $a = 1$

$$S_{\nu,N}(1) = 0.125/N \tag{24}$$

For other $\tilde{a} < 1$ we have calculated $S_{\nu,N}(\tilde{a})$ numerically. Figure 6 shows some examples. Though these $S_{\nu,N}(\tilde{a})$ vary over about ten orders of magnitude, round-off errors have no appreciable effect in this range as will become clear in the discussion of critical spectra below. To avoid spectral leakage[4,5] N has always been chosen an integer multiple of the underlying period p. Because of (19) $S_{\nu,N}$ has the symmetry

$$S_{\nu,N} = S_{N-\nu,N} \tag{25}$$

Therefore we only need to discuss $S_{\nu,N}$ in the interval $0 \leqslant \nu/N \leqslant 1/2$.

All spectra contain a continuum part due to the chaotic motion within the boxes and lines representing the underlying cycle. A cycle of period p causes lines to appear at $\nu/N = j/p$, $j = 1, 2, \ldots, p-1$. The relative magnitudes of these lines reflect the intrinsic structure of the cycle. (Compare for example Fig. 6b with Fig. 6e, and Figs. 6f, 6g, and 6h with each other.) Going from a cycle to its subharmonic adds a fine structure to the otherwise practically unchanged overall structure of the cycle. Therefore the already existing lines in the spectrum do hardly change in magnitude while new lines corresponding to the doubled period of the subharmonic appear (Figs. 6a–6d).

The small fluctuations on the continuum are due to the finite average used in the numerical computation. For primary cycles (Figs. 6e–6h) the continuum has practically no structure, whereas subharmonics have in most cases a strongly structured continuum (Figs. 6b–6d) with local extrema at the cycle frequencies j/p. The amplitude of this modulation is the

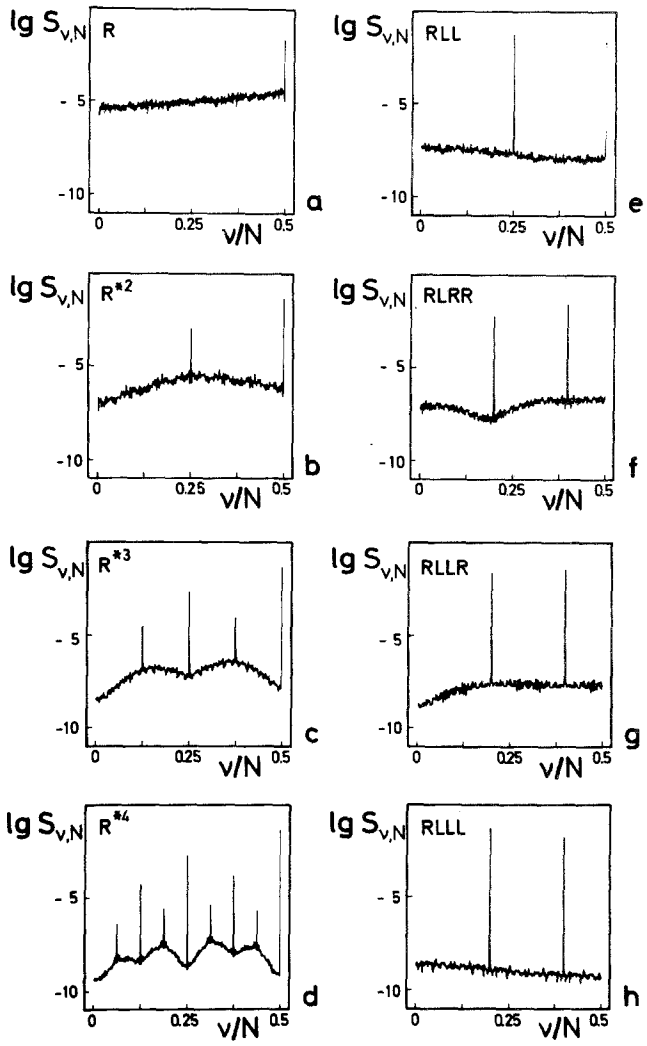

Fig. 6. Spectra of several states of periodic chaos.

larger the slower the envelopes of the c.f.'s approach their asymptotic values. Thus the strength of the modulation is to a certain extent a consequence of the increased correlation time observed in the box c.f.'s of subharmonics. The distance between the local minima of this modulation is just twice the frequency interval between neighboring lines corresponding to a peak in the c.f. at $\tau = p/2$. The occurrence of this peak is obviously

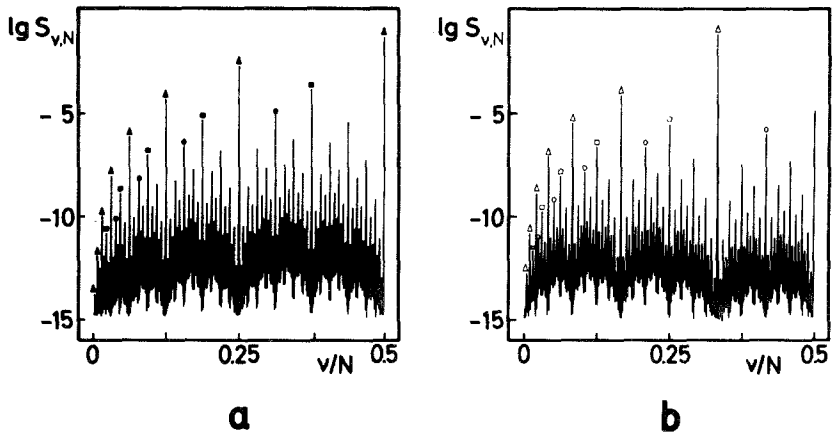

Fig. 7. Critical spectra. (a) $a = a_c^{(1)} = 0.892\,486\,417\ldots$; (b) $a = a_c^{(3)} = 0.962\,358\,420\ldots$; the symbols denote different line series $\nu_n = 2^{-n}\nu_0$.

due to the pairing of chaotic boxes characteristic for subharmonics. A closer inspection of the spectra of higher-order subharmonics reveals that this effect is also present, though less pronounced, for $\tau = p/4$, $\tau = p/8, \ldots$.

Considering subharmonics of increasingly higher order one obtains spectra which converge in an asymptotically self-similar fashion to the spectrum at the critical point $a_c^{(p)}$. In these critical spectra (Fig. 7) lines can be grouped into series. The intensity of lines in each series shows scaling behavior with the frequency.

Considering several line series of the form $\{S_{\nu_n,N} \mid \nu_n = 2^{-n}\nu_0, \nu_0, N$ fixed$\}$ we obtained

$$S_{\nu_n,N} \underset{n\to\infty}{\propto} (\nu_n/N)^{\tilde{\mu}} \tag{26}$$

with $\tilde{\mu} \cong 6.31$. (see Fig. 8). A calculation analogous to Ref. 13 relates $\tilde{\mu}$ to the scaling parameter α of the critical limit sets $\Lambda(a_c^{(p)})$:

$$\tilde{\mu} \cong 2ld\left[2\alpha^2/(\alpha - 1)\right] \tag{27}$$

i.e., $\tilde{\mu} \cong 6.12$. The difference between the experimental and the theoretical value is probably due to the approximative nature of the scaling assumption. Despite the variation of α on the limit set $\Lambda(a_c^{(p)})$ the data points in Fig. 8 form almost perfect straight lines in the low-frequency range. Only when intensities become smaller than $\sim 10^{-14}$ do deviations from linearity occur, which we attribute to round-off errors. Hence we conclude that our

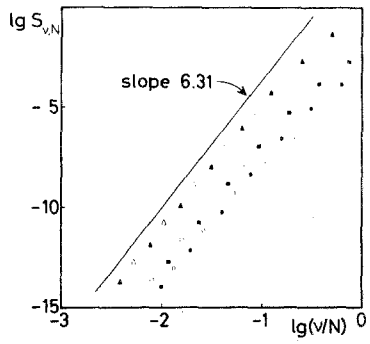

Fig. 8. Asymptotic scaling of intensities within several line series; the different symbols refer to the series marked in Fig. 7.

numerically computed spectra in Fig. 6 are not seriously affected by round-off errors.

6. APPROXIMATION FOR SPECTRA OF PERIODIC CHAOS

The spectra of periodic chaos can approximately be calculated by separating periodic and purely chaotic components. To this end we define a normalized sequence $\{\tilde{x}_\tau(\tilde{a})\}_{\tau=0}^{\infty}$ by

$$x_\tau(\tilde{a}) = \check{x}_\tau(\tilde{a}) + l_\tau(\tilde{a})\tilde{x}_\tau(\tilde{a}), \qquad \tau = 0, 1, 2, \ldots \tag{28}$$

where $x_0 \in I_0^{(p)}$ and $\{\check{x}_\tau(\tilde{a})\}_{\tau=0}^{\infty}$, $\{l_\tau(\tilde{a})\}_{\tau=0}^{\infty}$ are the sequences originating from the periodic continuation of the finite sets of instable fixed points and box lengths. These sequences contain the periodic components of $\{x_\tau(\tilde{a})\}_{\tau=0}^{\infty}$, whereas $\{\tilde{x}_\tau(\tilde{a})\}_{\tau=0}^{\infty}$ represents the chaotic part. Its subseries within each box have already been considered in (12). In terms of the decomposition (28) one obtains

$$\langle x_t \rangle = \langle \check{x}_t \rangle + \langle l_t \tilde{x}_t \rangle \tag{29}$$

$$\langle x_t x_{t+\tau} \rangle = \langle \check{x}_t \check{x}_{t+\tau} \rangle + \langle \check{x}_t l_{t+\tau} \tilde{x}_{t+\tau} \rangle + \langle \check{x}_{t+\tau} l_t \tilde{x}_t \rangle + \langle l_t l_{t+\tau} \tilde{x}_t \tilde{x}_{t+\tau} \rangle \tag{30}$$

Our approximation is based on two assumptions. The first one is the *decorrelation assumption*:

The chaotic component is not correlated with the periodic components.

The second assumption relates to the statistics of $\{\tilde{x}_\tau\}_{\tau=0}^{\infty}$. By the transformation (28) it is clear that $\{\tilde{x}_\tau\}_{\tau=0}^{\infty}$ is normalized to the unit interval. Considering for example the case $p = 3(RL)$, see Fig. 2a, this means the off-diagonal boxes $j = 0, 1, 2$ are transformed to the unit square

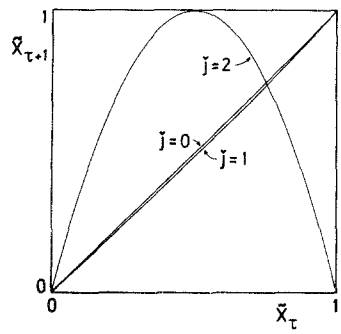

Fig. 9. The mappings within off-diagonal boxes $\check{j} = 0, 1, 2$ of Fig. 3a after the normalization transformation (28).

(Fig.9). While the map in $\check{j} = 2$ becomes the well-known parabola f_1, the maps in $\check{j} = 0, 1$ are transformed into maps close to the identity. For a general period-p chaos the normalized map in $\check{j} = p - 1$ is f_1 and the other maps are more or less identities. The sequence $\{\tilde{x}_\tau\}_{\tau=0}^{\infty}$ is generated by cyclic application of the normalized maps in $\check{j} = 0, 1, 2, \ldots, p - 1$. Since those in $\check{j} = 0, 1, 2, \ldots, p - 2$ are almost linear and the one in $\check{j} = p - 1$ is f_1 with $c_\tau(1)$ as given in (11), it is natural to expect the temporal behavior of $\{\tilde{x}_\tau\}_{\tau=0}^{\infty}$ to be similar to the behavior of $\{x_\tau(1)\}_{\tau=0}^{\infty}$ slowed down by a factor p. This leads to the *time dilation assumption*:

The c.f. of the normalized sequence $\{\tilde{x}_\tau\}_{\tau=0}^{\infty}$ of period-p chaos is given by

$$\tilde{c}_\tau(\tilde{a}^{(p)}) = \begin{cases} 0.125(1 - \tau/p) & \text{for } 0 \leqslant \tau \leqslant p \\ 0 & \text{for } p < \tau \end{cases} \tag{31}$$

and the mean value is

$$\langle \tilde{x}(\tilde{a}^{(p)}) \rangle = 0.5 \tag{32}$$

By means of these two assumptions we obtain from (29) and (30)

$$c_\tau(\tilde{a}^{(p)}) \cong c_\tau^*(\tilde{a}^{(p)}) + d_\tau(\tilde{a}^{(p)})\tilde{c}_\tau(\tilde{a}^{(p)}) \tag{33}$$

where c_τ^* is the c.f. of $\check{x}_\tau + \langle \tilde{x}_t \rangle l_\tau$ and

$$d_\tau(\tilde{a}^{(p)}) = \frac{1}{p} \sum_{t=0}^{p-1} l_t(\tilde{a}^{(p)}) l_{t+\tau}(\tilde{a}^{(p)}) \tag{34}$$

If N is an integer multiple of p, equation (33) is also valid for the respective N-truncated quantities. The Fourier transformation of (33) yields

$$S_{\nu,N}(\tilde{a}^{(p)}) \cong S_{\nu,N}^*(\tilde{a}^{(p)}) + \sum_{\mu=0}^{N-1} D_{\nu-\mu,N}(\tilde{a}^{(p)}) \tilde{S}_{\mu,N}(\tilde{a}^{(p)}) \tag{35}$$

where $S_{\nu,N}$, $S^*_{\nu,N}$, and $\tilde{S}_{\nu,N}$ are the spectra of the corresponding truncated correlation functions $c_{\tau,N}$, $c^*_{\tau,N}$, and $\tilde{c}_{\tau,N}$ and

$$D_{\nu,N}(\tilde{a}^{(p)}) = \frac{1}{N} \sum_{\tau=0}^{N-1} \exp(-i2\pi\nu\tau/N) d_{\tau,N}(\tilde{a}^{(p)}) \tag{36}$$

The results obtained with this approximation for the spectra in Fig. 6 are shown in Fig. 10. The agreement is fairly good. The largest errors occur

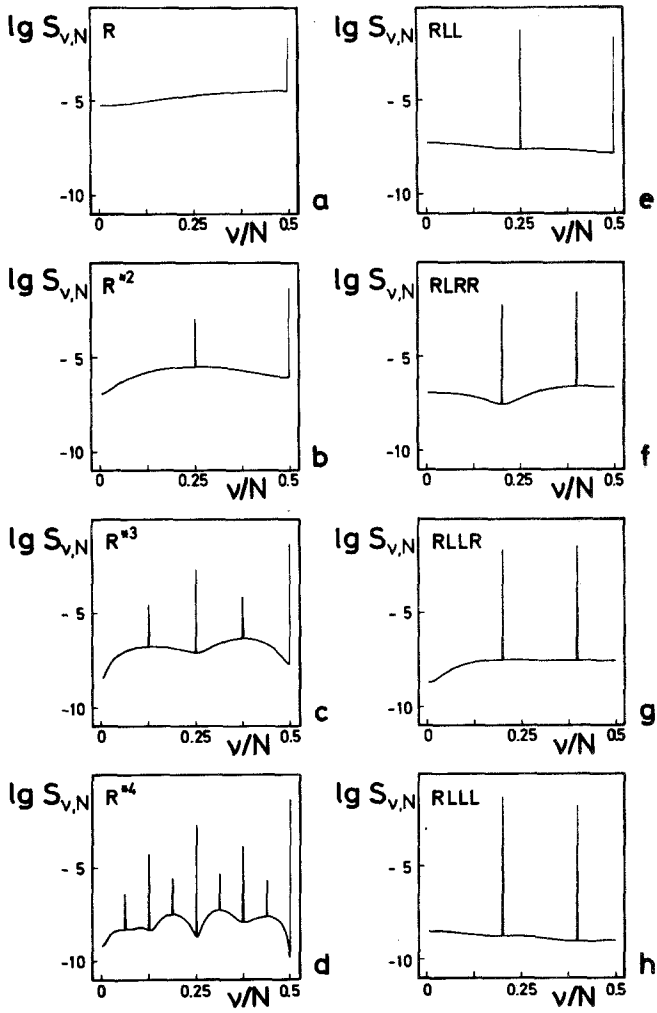

Fig. 10. Results obtained with (35) for the spectra of Fig. 6.

for the spectra of subharmonics since our approximation (31) does not account for the slower decay of box c.f.'s in this case.

When $\tilde{a}$ approaches a critical value $a_c^{(p)}$, (35) becomes an exact expression for the spectrum because

$$\lim_{\tilde{a} \to \tilde{a}_c} D_{\nu-\mu,N}(\tilde{a}) = 0 \tag{37}$$

and all the information about the dynamics is filled in via $S^*_{\nu,N}(a_c^{(p)})$.

Fujisaka and Yamada[46] used Mori's projector formalism to calculate c.f.'s of discrete chaotic processes. Hence their method requires as input information the invariant measure $\mu^{(p)}(x)$, which is frequently known for $p = 1$ but rarely for $p > 1$, whereas we use x_{j_2} l_j, $j = 0, 1, 2, \ldots, p-1$ and the c.f. $\check{c}_\tau$ of the normalized map in box $j = p - 1$. So, by using their method first to find $\check{c}_\tau$ and then applying the procedure described above the correlations and spectra of periodically chaotic states of dynamic laws different from (2) might be successfully approximated as well.

REFERENCES

1. R. M. May, *Nature* **261**:459 (1976).
2. M. J. Feigenbaum, *J. Stat. Phys.* **19**:25 (1978).
3. M. J. Feigenbaum, *J. Stat. Phys.* **21**:669 (1979).
4. P. Collet, J.-P. Eckmann, and O. E. Lanford III, *Commun. Math. Phys.* **76**:211 (1980).
5. P. Collet and J.-P. Eckmann, Properties of Continuous Maps of the Interval to Itself, in *Lecture Notes in Physics* Vol. 116 (Springer, Berlin-New York, 1980), pp. 331–339.
6. I. Gumowski and C. Mira, *Dynamique Chaotique* (Cepadues, Toulouse, 1980).
7. I. Gumowski and C. Mira, Recurrences and Discrete Dynamic Systems, *Lecture Notes in Mathematics* Vol. 809, A. Dold and B. Eckmann eds. (Springer, Berlin-New York, 1980).
8. P. Collet and J.-P. Eckmann, Iterated Maps on the Interval as Dynamical Systems, *Progress in Physics* Vol. 1, A. Jaffe and D. Ruelle eds. (Birkhäuser, Boston-Basel-Stuttgart, 1980).
9. Bifurcation Theory and Applications in Scientific Disciplines, *Annals of the New York Academy of Science* Vol. 316, O. Gurel and O. E. Rössler eds. (The New York Academy of Science, New York, 1979).
10. I. Gumowski and C. Mira, *Informatica* Vol. 76 (Bled, Yugoslavia, 1976).
11. Yu. N. Belyaev, A. A. Morakhov, S. A. Shcherbakov, and J. M. Yavorskaya, *JETP Lett.*, **29**:295 (1979).
12. A. Libchaber and J. Maurer, *J. Phys. (Paris), Colloque* **41**:C3-51 (1980).
13. M. J. Feigenbaum, *Phys. Lett.* **74A**:375 (1979).
14. M. J. Feigenbaum, *Commun. Math. Phys.* **77**:65 (1980).
15. C. Boldrighini and V. Franceschini, *Commun. Math. Phys.* **64**:159 (1979).
16. J.-M. Wersinger, J. M. Finn, and E. Ott, *Phys. Rev. Lett.* **44**:453 (1980).
17. B. A. Huberman and J. P. Crutchfield, *Phys. Rev. Lett.* **43**:1743 (1979).
18. H. Nagashima, Chaotic States in the Belousov-Zhabotinsky Reaction, (Preprint, 1980).
19. R. A. Schmitz, K. R. Graziani, and J. L. Hudson, *J. Chem. Phys.* **67**:3040 (1977).
20. R. M. May and G. F. Oster, *The American Naturalist* **110**:573 (1976).
21. Y. Oono and Y. Takahashi, *Progr. Theor. Phys.* **63**:1804 (1980).

22. T.-Y. Li and J. A. Yorke, *Am. Math. Monthly* **82**:985 (1975).
23. F. C. Hoppensteadt and J. M. Hyman, *SIAM J. Appl. Math.* **32**:73 (1977).
24. Y. Oono, T. Kohda, and H. Yamazaki, *J. Phys. Soc. Jpn* **48**:738 (1980).
25. P. Coullet and C. Tresser, *J. Phys. (Paris), Lett.* **41**:L-255 (1980).
26. S. Grossmann and S. Thomae, *Z. Naturforsch.* **32a**:1353 (1977).
27. O. E. Lanford III, Remarks on the accumulation of period-doubling bifurcations, *Lecture Notes in Physics* Vol. 116 (Springer, Berlin-New York, 1980) pp. 340–342.
28. P. Coullet and C. Tresser, *J. Phys. (Paris), Colloque* **39**:C5-25 (1978).
29. C. Tresser and P. Coullet, *C. R. Acad. Sc. Paris* **287A**:577 (1978).
30. J. Guckenheimer, *Ann. N.Y. Acad. Sci.* **316**:78 (1979).
31. N. Metropolis, M. L. Stein, and P. R. Stein, *J. Comb. Theor.* **(A)15**:25 (1973).
32. C. Zörnig, Abzweigungsprobleme bei diskreter Iteration, Diploma thesis (Marburg, 1979); cited in Ref. 6, p. 103f.
33. M. P. Fatou, *Bull. Soc. Math. France* **47**:161 (1919); **48**:33 (1920); **48**:208 (1920).
34. C. Julia, *J. Math. Pure Appl.* **4**:47 (1918).
35. A. N. Sarkovskii, *Ukr. Mat. Z.* **16**:61 (1964).
36. P. Štefan, *Commun. Math. Phys.* **54**:237 (1977).
37. B. Derrida, A. Gervois, and Y. Pomeau, *J. Phys.* **A12**:269 (1979).
38. J. Couot and C. Gillot, Equations fonctionelles des densités de mesures invariantes par un endomorphisme de [0, 1] et simulation numérique, in *Proceedings of Equadiff* 78, pp. 139–147, Florence (May 1978).
39. S. Thomae, Untersuchung der Pseudostochastik in den Lösungen einiger nichtlinearer Transformationen, Diploma thesis (Marburg, 1977).
40. G. Pianigiani, *Boll. U.M.I.* **16-A**:374 (1979).
41. D. Ruelle, *Commun. Math. Phys.* **55**:47 (1977).
42. M. Misiurewicz, Absolutely continuous measures for certain maps of an interval, *Publ. Math. IHES* (1980).
43. Y. Oono and M. Osikawa, *Progr. Theor. Phys.* **64**:54 (1980).
44. E. N. Lorenz, Noisy Periodicity and Reverse Bifurcation (Preprint 1980).
45. F. J. Harris, *Proc. IEEE* **66**:51 (1978).
46. H. Fujisaka and T. Yamada, *Z. Naturforsch.* **33a**:1455 (1978).